Phosphoric Acid Doped Polybenzimidazole Membrane for High Temperature PEM Fuel Cell

Dilek Ergun,[1] Yilser Devrim,[1] Nurcan Bac,[2] Inci Eroglu[1]

[1]*Chemical Engineering Department, Middle East Technical University, 06531 Ankara, Turkey*
[2]*Chemical Engineering Department, Yeditepe University, 34755 Istanbul, Turkey*

Received 3 August 2010; accepted 18 November 2011
DOI 10.1002/app.36507
Published online 22 January 2012 in Wiley Online Library (wileyonlinelibrary.com).

ABSTRACT: In the present study, phosphoric acid doped polybenzimidazole (PBI) membranes with potential applications in high temperature PEM fuel cells were investigated. PBI was synthesized by polycondensation of 3,3′-diaminobenzidine and isophtalic acid in polyphosphoric acid. The formation of PBI was validated by H^1-NMR and elemental analysis. PBI membranes were prepared by solution casting method and immersed in phosphoric acid in order to provide ionic conductivity. The phosphoric acid doped membranes were used to prepare membrane electrode assemblies (MEA) for PEMFC operation. Gas diffusion layer (GDL) spraying method was used to prepare the electrodes. In order to determine optimum electrode structure, the effect of electrode preparation technique on fuel cell performances was studied. Two methods were applied in which the binder differs in the catalyst ink. In the first method, 5 wt % PBI solution was used as the binder. In the second method, polyvinylidene fluoride (PVDF) was used in addition to PBI as the binder in the catalyst ink. The MEA were tested in a single cell operating at 100°C without need for humidification of reactant gases. The observed maximum power output was increased considerably from 0.015 to 0.072 W/cm^2 at 150°C when the binder of the catalyst was changed from PBI to PBI and PVDF mixture (PVDF : PBI = 3 : 1). A single cell was operated up to 160°C and the power outputs of 0.032 and 0.063 W/cm^2 were obtained at operating temperatures of 125 and 160°C, respectively. The PVDF : PBI ratio was 1 : 3 in the catalyst ink at both temperatures. © 2012 Wiley Periodicals, Inc. J Appl Polym Sci 124: E267–E277, 2012

Key words: synthesis of polybenzimidazole; phosphoric acid doped polybenzimidazole; membrane electrode assembly preparation; PVDF; high temperature PEM fuel cell

INTRODUCTION

Fuel cells continue to attract significant attention in recent years. They have lots of advantages compared to the conventional systems that produce electricity. Among the types of fuel cells, proton exchange membrane fuel cell (PEMFC) technology has drawn the most attention because of its simplicity, viability, pollution-free operation, and quick start up.[1] It is also a serious candidate for automotive applications. Generally, PEMFC operates between 60 and 80°C due to thermal limitations of the polymer electrolyte commonly used (i.e., Nafion).

However there are several advantages for operation at elevated temperatures in the range of 100–200°C. These advantages are; faster chemical kinetics at the electrode, simple thermal and water management, and heat utilization.[2] Another benefit of high temperature operation is the reduced catalyst poisoning by impurities in the fuel, such as CO and CO_2. This poisoning effect has been shown to be very temperature-dependent and it is less pronounced with increasing temperature. Therefore, recent studies are focused on the development of polymer electrolyte membranes for operation at temperatures above 100°C.[3]

Among various types of alternative high temperature polymer electrolyte membranes developed so far, phosphoric acid doped polybenzimidazole (poly [2,2-(*m*-phenylene)-5,5-bibenzimidazole]; PBI) was reported as one of the most promising candidate, possessing high proton conductivity, high thermal stability, and high fuel cell performance at temperatures up to 200°C.[4,5] PBI is a fully aromatic heterocyclic polymer. It has high chemical resistance and extremely high temperature stability; thus it does not ignite up to 600°C. It holds adequate mechanical stability in both dry and hydrated state.[6] It is synthesized by melt polycondensation[7] and solution polymerization method.[8] In solution polymerization; the reaction temperature (170–200°C) is lower and also temperature control is easier compared

Correspondence to: Y. Devrim (yilser@gmail.com).
Contract grant sponsor: The Scientific and Technological Research Council of Turkey (TUBITAK); contract grant number: 104M364.
Contract grant sponsor: Middle East Technical University Scientific Research; contract grant number: BAP-2008-03-04-07.

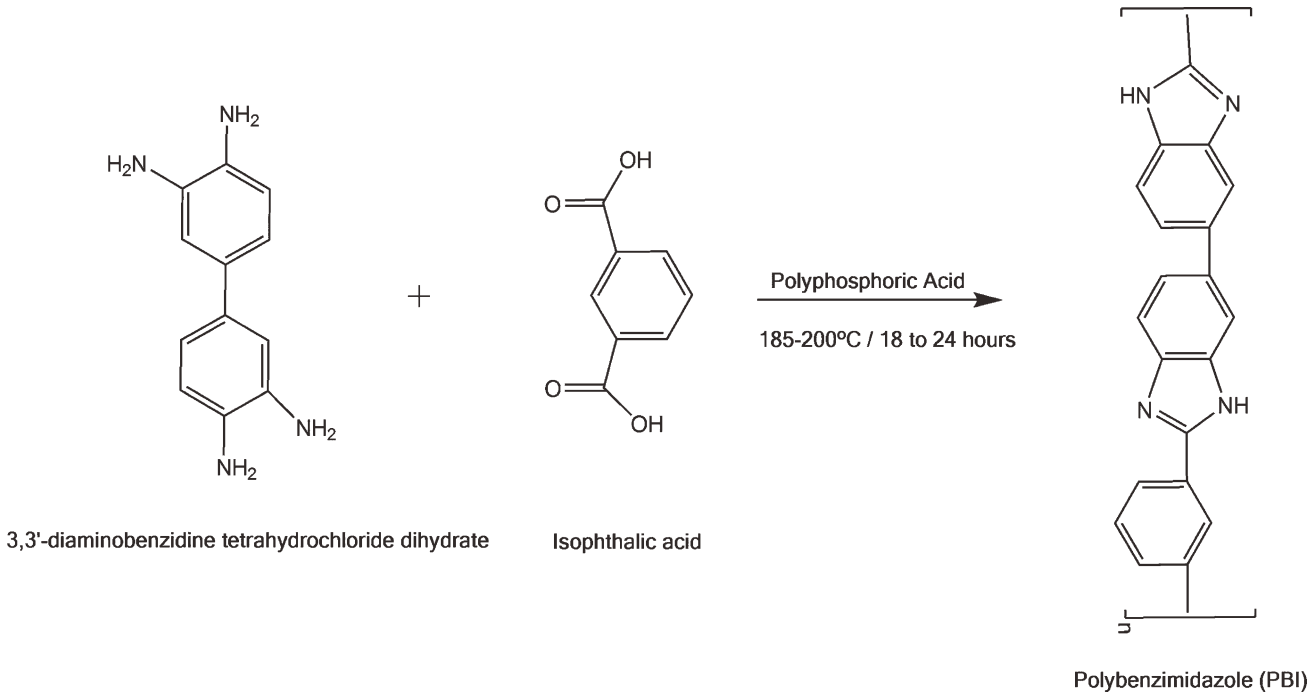

Scheme 1 Synthesis of PBI polymer.

to melt polycondensation method due to the used reaction solvent polyphosphoric acid (PPA).

The proton conductivity of pure PBI is low, but acid doping increases the proton conductivity remarkably, even in the anhydrous state.[9] PBI membrane can be doped with sulfuric acid, phosphoric acid, perchloric acid, nitric acid, and hydrochloric acid.[10] Phosphoric acid forms 3D hydrogen bonding network with PBI; therefore, it is the most promising doping material.[4] It has a high boiling point, therefore increases the thermal stability and proton conductivity of the PBI membranes.[11]

Phosphoric acid doped PBI membrane is operated in PEMFC without the need for humidification of reactant gases.[12] High doping level increases the proton conductivity of the PBI membrane, but decreases its mechanical stability. This effect is more pronounced at high temperatures.[2] Therefore, the phosphoric acid doping level and the molecular weight of PBI are the two critical parameters to be optimized.

There have been several reports of the synthesis of PBI derivatives and their application for PEMFC. Nevertheless, the research conducted so far has been limited to membranes, and only a few studies of electrode fabrication have been reported.[13,14] To enhance cell performance by an effective electrode fabrication is very important. This article presents an investigation of the effects of binding material in the catalyst layer on single-cell performance.

PBI polymer was synthesized with different molecular weight and membranes were prepared by solution casting and doped with phosphoric acid. Membrane electrode assemblies (MEA) were prepared by spraying on gas diffusion layer (GDL) by two methods in which the binder differs in the catalyst ink. The surface morphology of the electrodes and the cross-sections of the MEA were examined by scanning electron microscope (SEM) analysis. The performances of the PBI membranes were tested in a single cell.

EXPERIMENTAL

Materials

The monomers 3,3′-diaminobenzidine tetrahydrochloride (DAB.4HCl.2H_2O, 98%) and isophtalic acid (IPA, 99%) were obtained from Sigma-Aldrich) (USA). PPA (115%) was obtained from Merck (Germany) and it was used as received. *N-N* dimethylacetamide ($CH_3C(O)N(CH_3)_2$ DMAc), sulfuric acid (%98), and *o*-phosphoric acid (85%) were used as received. All solvents used were high grade reagents.

PBI synthesis and membrane preparation

PBI polymers were synthesized by solution polymerization method.[2,15] The monomers are DAB.4HCl.2H_2O and IPA and the solvent is PPA. The polymerization system consisted of a three necked flask with a mechanical stirrer, nitrogen inlet, and a $CaCl_2$ drying tube and it was controlled by a programmable temperature controller. The reaction scheme is given in Scheme 1.

PBI membranes were prepared by the solution casting method. PBI was dissolved in DMAc, and 3 wt % of LiCl was used as a stabilizer. The concentration of

the PBI solution was selected 10 wt %. In literature, the concentration of the PBI solution varies between 5 and 20 wt %. Below 5 wt %, the precipitation of polymer chains of PBI is not sufficient to form compact and complex helical structures for membrane formation; and above 20 wt %, it becomes impossible to obtain a homogeneous solution.[16] The solution was mixed in an ultrasonic bath at 80°C and also magnetically stirred. The homogeneous solution was cast onto petri dishes. The thickness and the size of the membranes were varied by controlling the volume of the solution and the diameter of the petri dishes. After casting, DMAc was evaporated in a ventilated oven in a temperature range from 80 to 120°C for 24 h. Finally, the membranes were immersed into boiling deionized water for 5 h to remove LiCl. A final drying step is applied at 190°C to remove any traces of the solvent. The thickness of the PBI membranes was controlled between 70 and 80 μm.

The PBI membranes were immersed into phosphoric acid solutions with different concentrations (75–85%). They were left at least 2 weeks in the acid. The weight gain due to both water and phosphoric acid was estimated by comparing the weight change before and after the doping process. The acid is absorbed in the membrane structure due to the strong interaction between PBI and phosphoric acid. The acid doping level was quantified by the number equal to the number of absorbed phosphoric acid molecules per repeat unit of PBI and calculated according to the following equation:

$$\text{Acid doping level} = \frac{\text{Weight difference}}{\text{Initial weight}} \times \frac{M_w \text{ of PBI repeat unit}}{M_w \text{ of } H_3PO_4} \quad (1)$$

Polymer and membrane characterization

The H^1-NMR spectra of PBI were recorded on a Bruker (300 MHz) spectrometer with Dimethyl sulfoxide (DMSO-d_6) as a solvent. The composition of the elements (C, H, and N) in the PBI structure were analyzed by elemental analysis (LECO, CHNS-932).

The molecular weight of the synthesized polymers was determined by the Ubbelohde viscometer method. Four solutions of 0.25, 0.5, 0.75, and 1 g/dL PBI in 98% (wt) sulfuric acid were prepared. Efflux times of all the solutions and the pure solvent were measured at 30°C in an Ubbelohde viscometer. The intrinsic viscosity, [η], is related with the weight-averaged molecular weight, M_w, is given by the Mark Houwink equation as follows;

$$[\eta] = K(M_w)^a \quad (2)$$

where K, a are constants that depend on the temperature, solvent type, and the type of the polymer. $K = 1.94 \times 10^{-4}$ and $a = 0.791$.[17]

Thermal stability of the PBI membrane was examined for the temperature range of 25–700°C at a heating rate of 10 °C/min under nitrogen atmosphere using a Thermal Analyzer (DuPont TA 951).

The X-ray powder diffraction (XRD) analysis was performed using an X-ray diffractometer (Rigaku D-MAX 2200, Japan) with CuK_α ($\lambda = 1.5406$ Å) radiation over the range $5^\circ \leq 2\theta \leq 100^\circ$.

Mechanical strength of the phosphoric acid doped and undoped membranes was measured with a vertical film device (INSTRON 3367) with a constant stretching speed of 5 mm/min at room temperature with a relative humidity (RH) of 30%. A minimum of five specimens was tested for each sample.

Membrane electrode assembly preparation

MEA were prepared by spraying catalyst ink on to the GDL (31 BC, SGL Carbon, Germany).[18] Firstly, the catalyst ink that is composed of catalyst (20 wt % Pt/C), solvent (DMAc) and the binder (PBI : polyvinylidene fluoride (PVDF)) was prepared by mixing the contents in an ultrasonic bath. The ink was sprayed onto the GDLs until the required Pt loading was attained (0.4 mg Pt/cm^2 for both anode and cathode sides). The catalyst loading was controlled by weighing the GDLs at different times. After the catalyst ink was sprayed onto the GDL, the electrodes were kept in the oven at 190°C for 3 h to remove any solvent traces. Finally, the electrodes were hot pressed onto both sides of the phosphoric acid doped PBI membrane (7 mol phosphoric acid molecules/repeating unit of PBI) at 150°C and 172 N/cm^2 for 10 min. In this study; two MEA preparation methods were developed.

In the first method, 5 wt % PBI solution was added to the catalyst ink as binder. After preparation, the electrode was impregnated with phosphoric acid and the PBI in the catalytic later was doped to enhance the ionic contact.[11] In the second method, PVDF was added to PBI and the mixture is used as the binder in the catalyst ink. After preparation, these electrodes were not doped with acid since PVDF provides the ionic contact. MEA were prepared from these electrodes by hot pressing them onto both sides of the phosphoric acid doped PBI membranes. The mechanical strength, electrical properties, and temperature resistance properties of the binders are given Table I.[18,19] Phosphoric acid doped PBI membrane is used for MEA preparation.

Surface morphology of the electrodes

The surface morphology of electrodes and cross-sectional scans of the MEA were examined in QUANTA 400F Field Emission Scanning Electrode Microscope using both secondary electron (SE) and

TABLE I
The Mechanical Strength, Electrical Properties, and Temperature Resistance Properties of the Binders

Binder	Tensile strength (MPa)	Elongation (%)	Dielectric constant at 1 MHz	Thermal conductivity × 10^{-4} (cal/cm sec °C)	T_g[a] (°C)	T_d[b] (°C)
PBI	96	20	4.20	9.64	400	720
PVDF	42.8	43	8.5	3.0	−35	390

[a] Glass transition temperature.
[b] Degradation temperature.

back-scattered electron (BSE) modes under similar experimental conditions: same current of primary beam scan rates, and pixel resolution. In order to obtain high quality SEM images of the cross-section, the MEA were broken immediately after dipping in liquid nitrogen.

PEM fuel cell performance tests

The finished MEA with an active area of 5 cm^2 were tested in a fuel cell test station built at METU Fuel Cell Technology Laboratory. A single PEM fuel cell (Electrochem, FC05-01SP-REF) was used in the experiments. The fabricated power of the cell was manipulated by an electronic load (Dynaload_RBL488), which can be controlled either manually or by the computer. The current and voltage of the cell were monitored and logged throughout the operation of the cell by the fuel cell test software (FCPower v. 2.1.102 Fideris). The fabricated MEA was placed in the test cell and the bolts were tightened with a torque of 1.7 N m on each bolt. In the test station, oxygen and hydrogen were used as oxidant and fuel, respectively. The reactant gases were fed to the fuel cell through Aalborg-171 mass flow controllers at a rate of 0.1 slpm. Prior to entering the fuel cell, the gases were transferred through the stainless steel gas lines and heated with resistance heaters. Proportional Integral Derivative (PID) temperature controllers were used to operate the system at a required temperature. The cell was operated at 0.5 V until it came to steady state. After steady state was achieved, starting with the open circuit voltage (OCV) value, the current–voltage data were logged by changing the load.

RESULTS AND DISCUSSION

Characterization of PBI polymer

The formation of PBI polymer was confirmed by the H^1-NMR spectra as shown in Figure 1. In Figure 1, the imidazole proton peak was observed at 13.3 ppm, and all the aromatic protons were at 7–10 ppm. The composition of the C, H, and N in the PBI structure was analyzed by elemental analysis. The theoretical percentages of C, H, and N of the polymer are, respectively, 77.92, 3.9, and 18.18 and the experimental results were 72.14, 4.5, and 17.66. The difference belongs to experimental errors which are ~ 5%. It is known that phosphoric acid-doped PBI is very hygroscopic. During the sample preparation and handling for elemental analysis, the PBI absorbed water from air.[20] The residual percentage due to the oxygen element in the structure is caused by absorbed water throughout the analysis. This absorption justifies the decrease of the C and N percentages and also the increase of the H percentage of the experimental result. The experimental percentages of C, H, and N (on dry base) of the polymer are 77.92, 3.9, and 18.18, respectively. The elemental analysis on dry base was performed for confirmation several times and the same percentages values were obtained for each experiment.

It is known that a higher molecular weight leads to a higher mechanical strength and a better chemical stability for polymeric membranes.[9–11,16] Thus, a long lifetime of the PEMFC is related to the chemical resistance to radicals HO· and HO_2· generated during the fuel cell operation (in the anode by the oxygen permeated through the membrane and in the cathode during the O_2 reduction). Molecular weights change due to the reaction conditions are shown in Table II. The parameters that affect molecular weight are reaction time and reaction temperature.

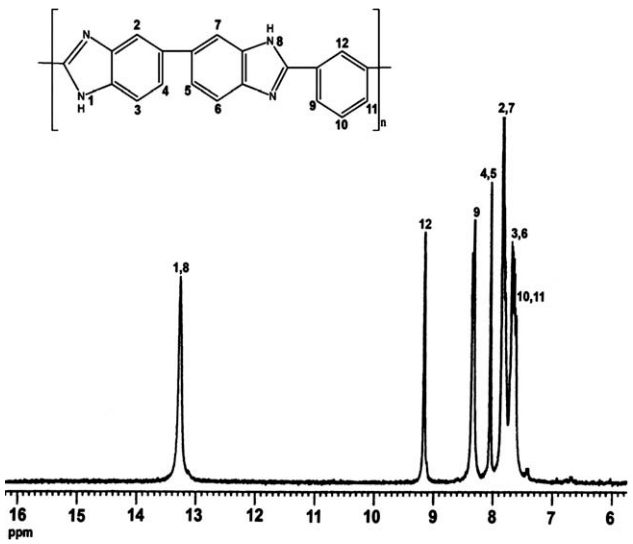

Figure 1 ^{1}H-NMR spectra of PBI polymer.

TABLE II
The Effect of Synthesis Conditions on the Molecular Weight and Intrinsic Viscosity of PBI Polymer Produced

Synthesis No	Reaction temperature (°C)	Reaction time, (h)	Intrinsic viscosity, (dL/g)	Molecular weight
1	170–200[a]	24	2.00	118,500
2	200	24	1.89	111,000
3	200	18	1.48	81,200
4	185	18	0.46	18,700

[a] Reaction was started at 170°C and continued at 170°C for 4 h. Then the temperature was increased to 200°C at a heating rate of 2 °C/min, and the reaction was continued at 200°C for 20 h.

Molecular weight decreases by decreasing the synthesis temperature and also the reaction time. High molecular weight is a required property for the polymer, because increased acid doping levels are possible. But at high doping levels the mechanical strength of the membrane became poor. A molecular weight higher than 18,000 seems to be necessary for sufficient conductivity and mechanical strength of the membranes.[21]

Thus, it is important to work with a polymer with an adequate molecular weight. By increasing the temperature from 185°C to 200°C, molecular weight was increased from 18,700 to 81,200. At a reaction temperature of 200°C, the molecular weight increased from 81,200 to 111,000 by increasing reaction time from 18 to 24 h. A two-step solution polymerization (1st step at 170°C and 2nd step at 200°C) has resulted in a PBI product with the highest molecular weight (118,500). The reproducibility analyses of the molecular weight measurement were done and ±3% error was observed.

XRD analysis and thermal properties PBI membranes

PBI has a semi-crystalline structure. The crystallinity is observed by XRD analysis of H_3PO_4 doped and undoped PBI membranes (Fig. 2). In the XRD spectra of PBI membrane there is only a single broad peak at about 25°. The peak at 25° corresponds to the spacing between two parallel benzimidazole chains. Wereta and Gehatia observed the parallel stacking of the benzimidazole rings to the film surface (parallel orientation).[22] However, there is no peak corresponding to LiCl $2\theta = 20.10°$ and 36.96° which disappear with LiCl.[23] When the membranes were doped with the H_3PO_4, the residual crystalline order is completely destroyed. The films were more amorphous for higher doping content. The observed spectra were in agreement with the results of the literature.[24]

The thermal stability of undoped and doped PBI membranes have been studied by thermogravimetric analysis. As seen from Figure 3, for undoped PBI, no weight loss occurs at temperature up to 400°C, indicating the excellent stability of PBI polymer. For the phosphoric acid doped PBI membrane, about 13% weight loss occurs at temperatures up to 400°C due to the dehydration of doped phosphoric acid. After this loss, the next dehydration step of the acid is observed above 600°C. The final weight loss around 800°C is assigned to the degradation of the polymer main chain.[25]

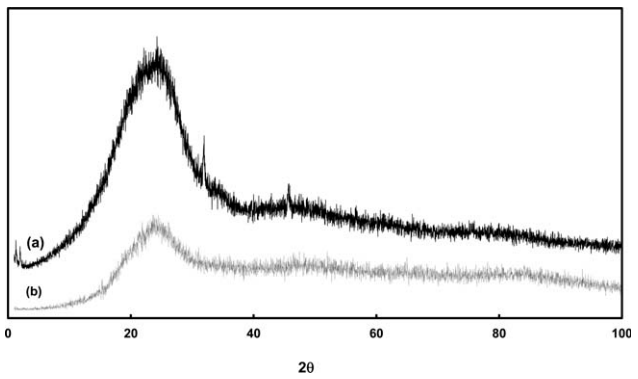

Figure 2 XRD spectra of (a) undoped and (b) H_3PO_4 doped PBI membranes.

Mechanical properties of doped and undoped PBI membranes

PBI mechanical properties have been reported to be highly dependent on the molecular weight.[5] The mechanical strength of the pure PBI membranes is determined by the hydrogen bonding between —N= and —NH— groups. When the membranes are treated with phosphoric acid stronger hydrogen

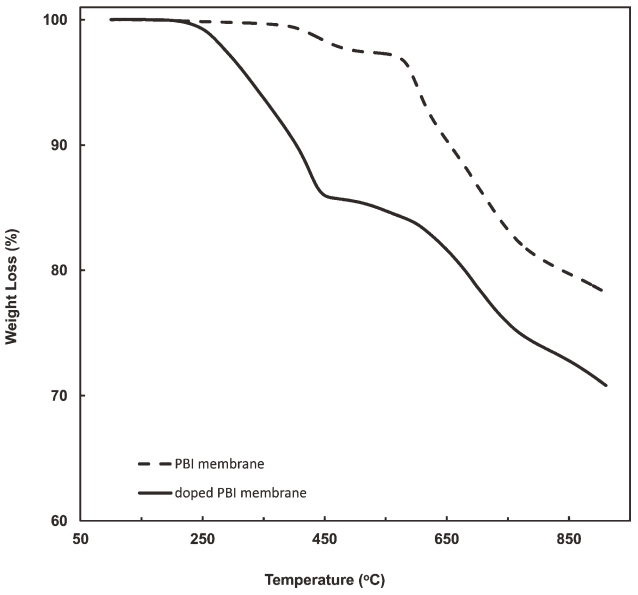

Figure 3 TGA analysis of undoped and doped PBI membranes.

TABLE III
Stress at Break and Elongation Data of Phosphoric Acid Doped PBI Membranes

Membrane doping level[a]	M_w	Stress at break[b] (MPa)	Elongation (%)
7	18,700	5.5	12
7	81,200	31	91
7	111,000	33	424
9	111,000	16	284
12	111,000	11	219

[a] Molecules of H_3PO_4/repeating unit of PBI.
[b] Measurements performed at room temperature and relative humidity.

bonds between —N= and phosphoric acid molecules are formed.[21] Generally, the mechanical strength of polymer membranes results from attractive forces between polymer molecules. Among the forces dipole–dipole interaction is mostly much stronger than London forces and induction interactions. But, when the molecular weight increases, London forces and induction interactions become increasingly significant.[26] Consequently, the higher molecular weighted polymer has better mechanical strength.

The significant effect of molecular weight on mechanical strength was observed by mechanical analysis. Table III displays the variation of the mechanical properties, measured from the stress at break for different doping levels and molecular weights.

The membrane cast from the polymer with a molecular weight of 18,700 has a stress at break value of 5.5 MPa, while the value is 33 MPa when the molecular weight increased to 111,000 (both membranes were doped with 7 molecules of H_3PO_4/repeating unit of PBI). A negligible decrease was observed when molecular weight decreased from 111,000 to 81,200.

When PBI membrane is doped with phosphoric acid, at doping levels higher than 2, the addition of free acids causes an important deterioration of its mechanical properties.[2] When phosphoric acid is introduced in massive amounts in the membrane, free acids get into the matrix and cause a volume swelling, separation of the PBI polymer chains, with the consequent reduction in the intermolecular forces.[21]

When the effect of the doping level is examined, it can be seen that for the membrane cast from the polymer with the highest molecular weight, the stress at break value decreased from 33 MPa at a doping level of 7–11 MPa at a doping level of 12. When PBI is impregnated with phosphoric acid, it undergoes an important deterioration of its mechanical properties. As expected, when the doping level increases, the stress at break decreases. When the doping level was above 7 for a molecular weight of 18,700, the stress at break determination was extremely difficult because of lower detection limit of the device used. The reduction of the films mechanical properties when impregnated with the acid and their enhancement with the increase in the molecular weight are clearly observed within this study. Mechanical analysis results are in agreement with literature.[27–30]

Surface morphology of the electrode and MEA

Both the surface morphology of the electrodes and the cross-sectional scans of the MEA were examined with a SEM. Top-view SEM images of the nondoped electrode prepared by the 1st method with a magnification of 100 and 50,000 are presented in Figure 4(a,b), respectively. The mud crack morphology for the electrodes can be seen from Figure 4(a). In the 1st method, the catalyst ink is composed of Pt, PBI, and DMAc. When the catalyst ink is applied to the GDL at a temperature of 100°C, the surface is dried to remove solvent and simultaneously create the pore structure of the catalyst layer. The top of the layer dries first and then the solvent vaporizes from the lower regions break through the top, to cause cracking. Seland et al. also report that the mud crack morphology of undoped electrodes appeared by spraying method.[31] Due to this mud cracked structure, substantial amount of catalyst is being forced into the crevices when spraying the catalyst layer. The catalyst that entered through the crevices will not contribute to the cell performance. Furthermore, cracks may increase the resistance in the catalyst layer to electron and proton transport during the fuel cell performances. Cracked areas will then have higher heat losses that, in turn, may increase the risk of membrane pinhole formation.[32]

The effect of the doping phosphoric acid on electrode surface can be seen clearly from Figure 4(c,d). Phosphoric acid covers all the surface of the electrode and penetrates into the pores of electrodes. Phosphoric acid covers the entire surface of the electrode and blocks off the cracks. So, gases may not be able to penetrate as deeply into catalyst and thus decrease the fuel cell performance.

In the 2nd method, PVDF is added additionally to the catalyst ink. Figure 4(e,f) shows the SEM images of the electrode which is prepared by the 2nd method as explained in the Experimental section. As seen in Figure 4(e), the surface of the electrode does not have any crevices; since the presence of PVDF prevents the cracking of the surface. Park et al. have reported similar results for PVDF using GDL preparation.[33] Figure 4(f) shows the uniform porous structure of the electrode. Ionomer clusters are formed on the electrode if carbon agglomerates are not well dispersed during the mixing stage or if too much ionomer is used in the ink. But there is no ionomer cluster on the prepared electrode.

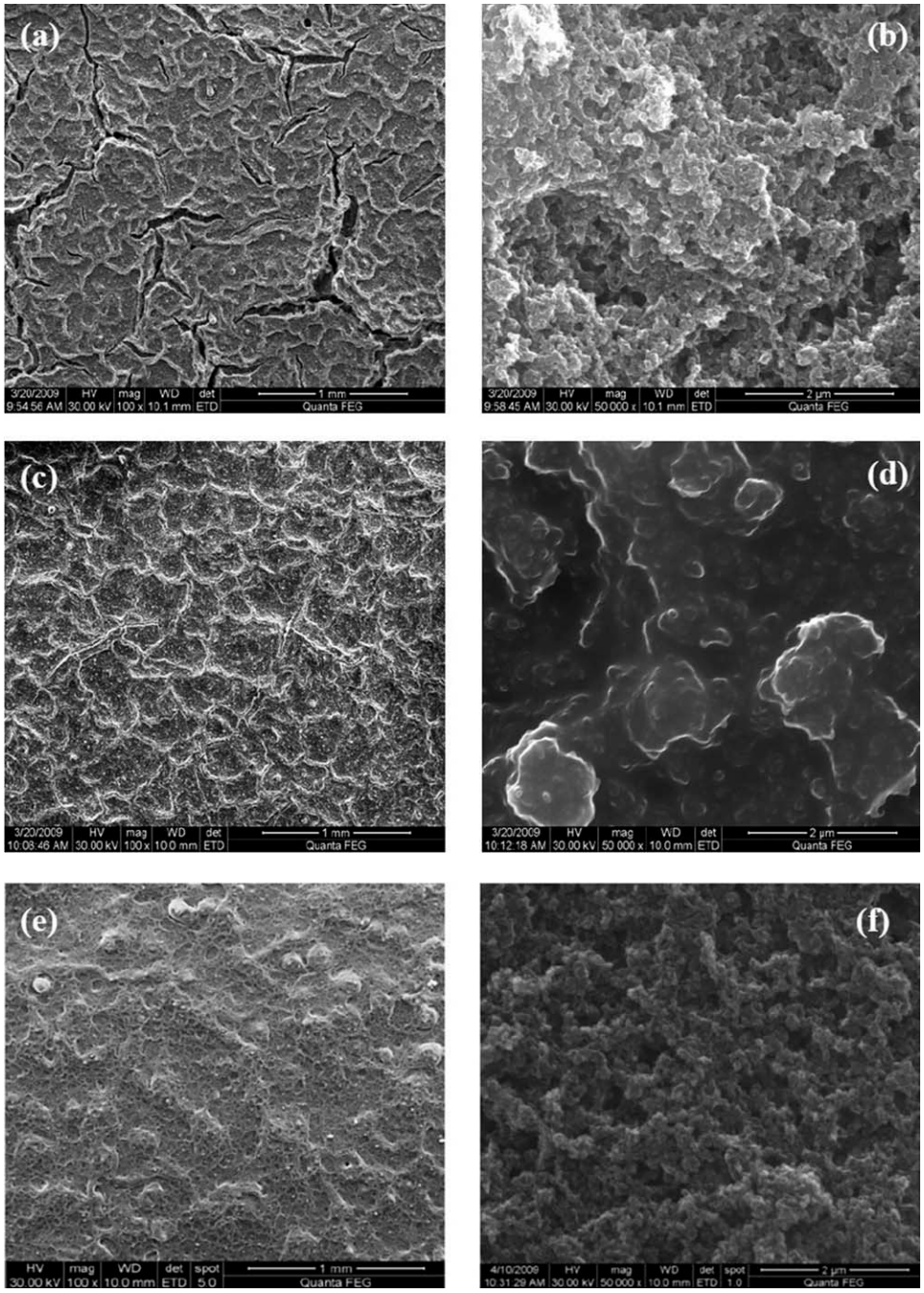

Figure 4 SEM images of non-doped electrode surface (prepared by Method 1); with a magnification of (a) 100×, (b) 50,000×; H_3PO_4 doped electrode surface (prepared by Method 1) with a magnification of (c) 100×, (d) 50,000×; and non-doped electrode (prepared by Method 2) with a magnification of (e) 100×, (f) 50,000×.

SEM images of cross-sections of the MEA examined before and after testing in PEM fuel cell in backscattered modes are shown in Figure 5. Backscatter mode was preferred as the catalyst layer can be seen easily since platinum shines up due to its high atomic weight. Figure 5(a) shows the cross-sectional view of the MEA before fuel cell testing. The catalyst layer can be seen as narrow bright bands on both sides of the membrane. The carbon support layer can also be identified easily as the dark region on the outside of the catalyst layer. The cross-section of both catalyst layers indicates that Pt catalyst was uniformly distributed. The interfaces between the PBI membrane and the electrodes can be observed in the image. No gaps between the membrane and electrodes are observed. SEM images of the cross-section of the respective MEA provide estimates of the real thickness of the catalyst layer and also membrane thickness. The overall thickness of the catalyst layer and the membrane were measured using the

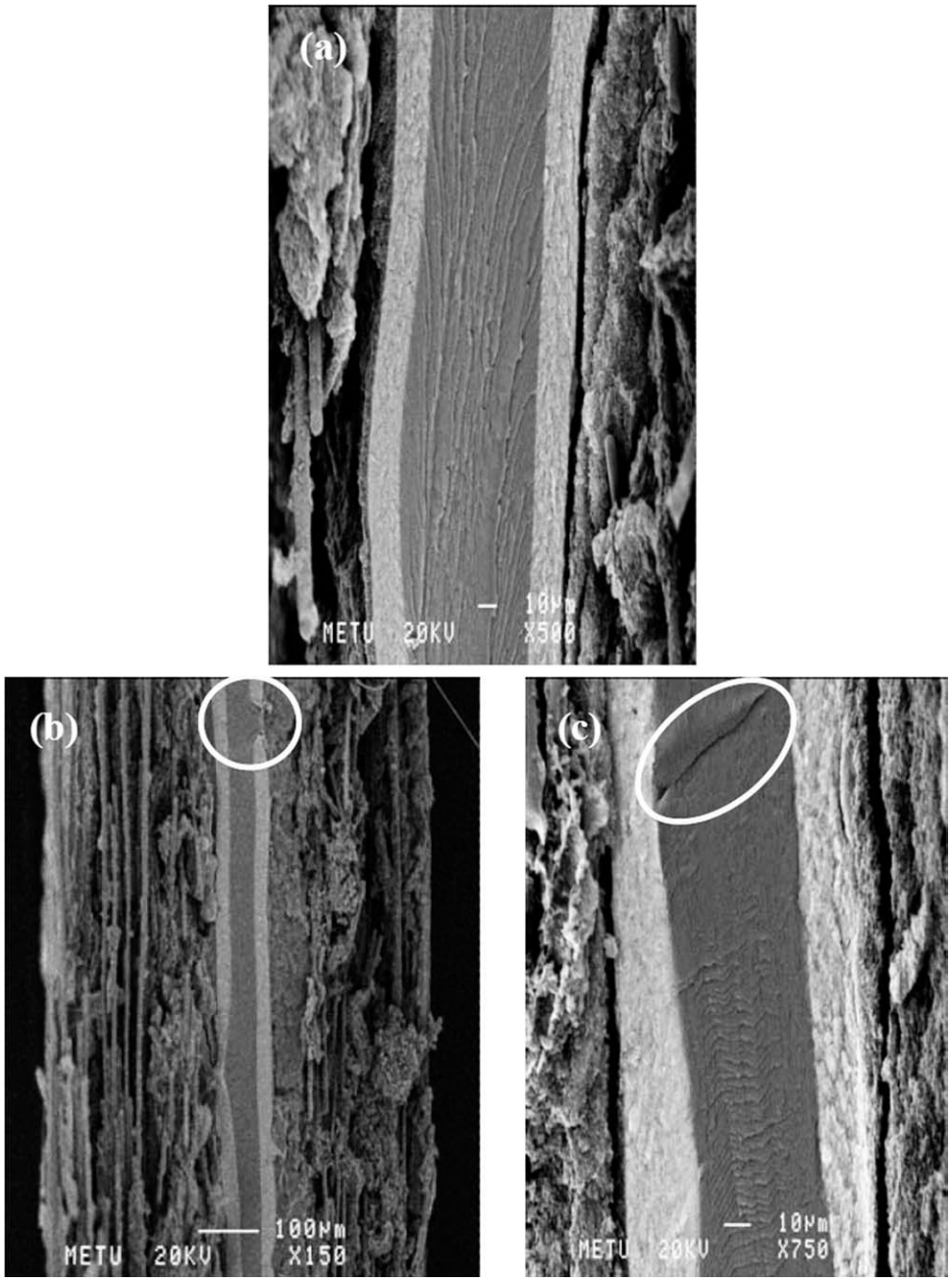

Figure 5 SEM images of the cross-sections of the MEA prepared by Method 2: (a) unused MEA, (b) deformation occurred on the catalyst layer after testing MEA in PEMFC, and (c) deformation occurred on the membrane layer after testing MEA in PEMFC.

SEM images [Fig. 5(a)] and found to be 20 and 70 μm, respectively. The membrane thickness was measured using the SEM image with a difference of ± 5 μm which may be due to hot pressing. SEM scans also show the reproducibility of the spraying technique. Deformation on the catalyst layer and the membrane cross-section are seen clearly in Figure 5(b,c), respectively. Catalyst layer deformations may occur due to carbon corrosion which is prone to oxidation in the presence of Pt.[34] On the other hand, it is known that the attack of HO· and HO_2· radicals produced by the incomplete reduction of oxygen on the cathode side is the main factor for the oxidative degradation of the PBI membrane.[35]

Fuel cell performances

Generally, the acid doping level is adjusted at 3.5–7.5.[28] In the present study, the doping level was fixed at 7. To achieve the required phosphoric acid doping level, it is advantageous to cast the membrane from a PBI polymer with a high molecular weight. Because in high molecular weight polymer,

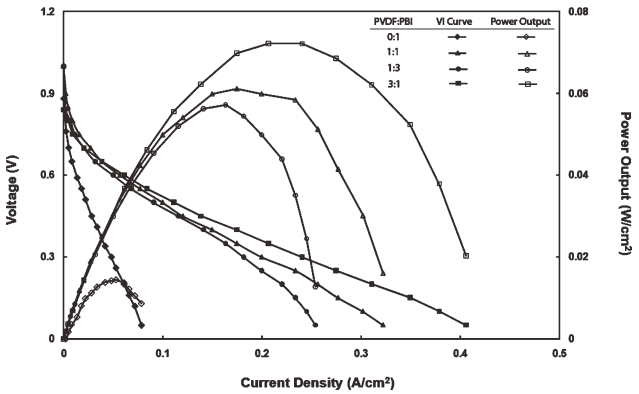

Figure 6 PBI performance curves of electrodes prepared by Method 1 and Method 2 at 150°C.

the number of bonded phosphoric acid molecules is more and free acids that reduces the mechanical strength are less than the case of low molecular weight. Throughout the study, the highest molecular weights obtained are 118,500 and 111,000, but these polymers had some difficulties in dissolution in DMAc. So the membranes which are cast from polymers with molecular weights of 81,200 were used for performance analysis.

The MEA prepared were placed in the PEM fuel cell with an active area of 5 cm^2. The operating temperatures of the cell and gas transfer lines were set to the required values. Before feeding of reaction gases, nitrogen was fed to the anode for 10–15 min to check whether there is a leakage through the membrane. After the nitrogen test, dry hydrogen and oxygen gases were fed to the anode and cathode sides of the cell, respectively, at a flow rate of 0.1 slpm. The effects of the binder used in the catalyst ink and operating temperature were studied throughout this study.

Effect of binder used in the catalyst ink on PEMFC performance

The performance curves of the MEA prepared by different binders are shown in Figure 6. The maximum power reached for the cell was 0.015 W/cm^2 at 150°C for the phosphoric acid doped electrodes (with MEA prepared by Method 1). The electrodes were doped with phosphoric acid to make an ionic contact between the membrane and electrodes. But this type of electrodes has a mud crack morphology which is explained in SEM analysis. Due to this mud cracked structure, a substantial amount of catalyst is being forced into the crevices when spraying the catalyst layer and phosphoric acid deteriorates the surface of the electrode since the surface is covered with the acid film that blocks the pores. When Method 2 was applied to the MEA (PVDF : PBI = 3:1), maximum power reached for the cell was increased considerably to 0.072 W/cm^2 at 150°C.

In performance analysis, the effect of the PVDF amount in the catalyst ink was also observed. The maximum power reached for the cell constructed with MEA prepared by Method 2 was 0.057, 0.061, and 0.072 W/cm^2 for the ratio of PVDF to PBI changed from 1 : 3 to 1 : 1 and 3 : 1, respectively. So it is clear that PVDF in the catalyst ink has an effect to increase the performance. Although the maximum power was observed at a PVDF : PBI ratio of 3 : 1, OCV value was decreased to 0.84 V, as shown in Figure 6. The decrease of the OCV and low current performance are caused by hydrogen crossover that causes the mixing of the reactant species before they have had a chance to participate in the electrochemical reaction.[36]

The influence of the PBI–H_3PO_4 loading in the catalytic layer of the cathode (referred as C/PBI weight ratio) on the fuel cell performance has been reported by Lobato et al.[37] A lower C/PBI weight ratio (higher PBI loading) has reduced the electrochemically available active area, and also, the reduced porosity of the electrode has limited the mass transfer processes, leading to the inferior performance. They have achieved the best results with a C/PBI weight ratio of 20, for both the anode and the cathode. In the present study, C/PBI ratio was fixed at 4, and this parameter should be considered in future studies.

Effect of operating temperature on PEMFC performance

The effect of temperature is very important for fuel cell performances. In general, a higher cell temperature results in a higher cell potential for PBI membranes. This is because of the fact that voltage losses in operating fuel cells decrease with temperature.

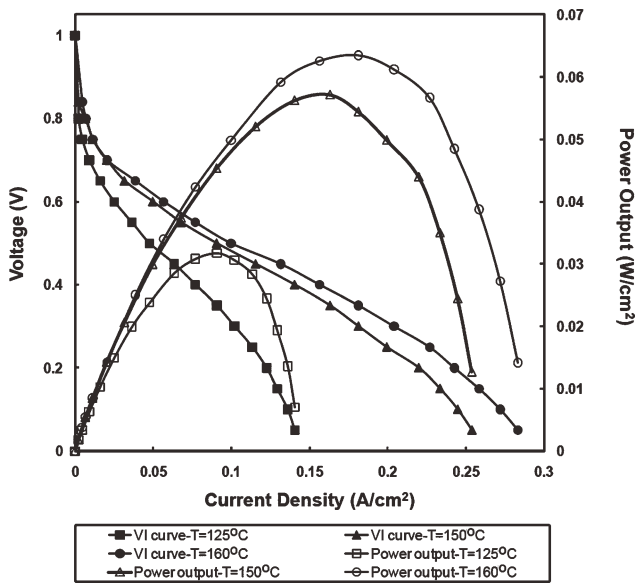

Figure 7 PBI performance curves of electrodes prepared by Method 2 with a PVDF : PBI ratio of 1 : 3, for different operating temperatures.

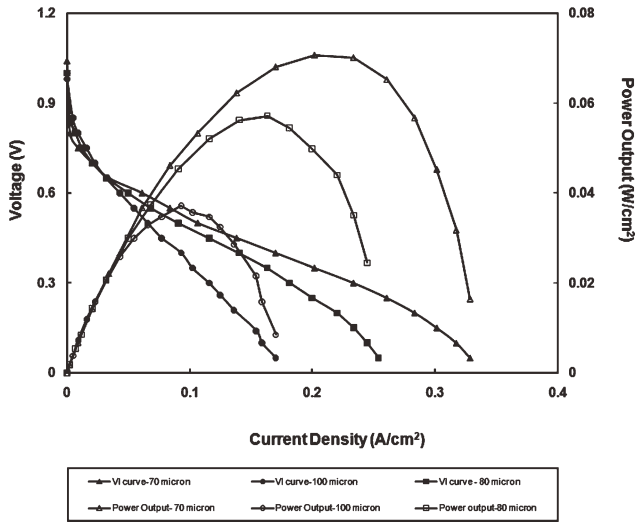

Figure 8 Effect of PBI membrane thickness on the performance of PEMFC at 150°C.

Open circuit potential of the membrane was 1 V which was quite acceptable for PEM fuel cells as stated in the literature as 0.90 V,[23] 0.87 V,[38] and 0.85 V.[11] As seen from Figure 7, fuel cell has reached to the maximum power outputs of 0.032 and 0.063 W/cm^2 when the fuel cell operating temperatures were at 125°C and 160°C, respectively, (MEA were prepared by Method 2 with a PVDF : PBI ratio of 1 : 3). It can be seen that the performance gets better at higher temperatures due to the higher electrolyte conductivity and the faster electrochemical reaction processes. Kongstein et al. observed a nearly linear increase of power density with increasing temperature, indicating the benefit of high-temperature operation.[11] For higher performance of the PBI membranes; operation at higher temperatures and also higher catalyst loadings of electrodes will be a focus of our on-going studies.

Effect of membrane thickness on PEMFC performance

The thickness of the membrane has also a serious effect on the performance and the thickness of the PBI membrane is varying from one research group to the other.[39–41] As it is seen from Figure 8, the single-cell test presents a current density of 56 mA/cm^2 and 43 mA/cm^2 at a cell voltage of 0.6 V with membrane thicknesses of 70 and 100 μm, respectively (MEA were prepared by Method 2). The better performances obtained with thinner membranes is an expected result as the proton transfer from anode to cathode gets easier as the membrane becomes thinner. A thin membrane clearly enhances the performance at lower potentials while a thick membrane would supposedly show better results at higher potentials where the current density is low.

CONCLUSIONS

In the present work, PBI was successfully synthesized by solution polymerization method. The molecular weight of the polymer was controlled in the range of 18,700–118,500 by changing the synthesis conditions, the reaction time, and temperature (185–200°C). H-NMR and elemental analysis results validated that the required polymer structure was obtained. As a result of mechanical analysis it is clearly seen that the mechanical strength of the PBI membrane increases with increasing molecular weight of polymer. It is also proved that phosphoric acid doping level is a critical parameter for the mechanical characteristics of the PBI membrane. The results showed that the mechanical strength decreases by increasing doping level due to volume swelling of the membrane caused by acid doping. The technique developed during the present work, to spray the catalyst ink onto GDL, is an appropriate method for the preparation of the electrodes. It should be emphasized that the binder of the catalyst is an important factor to achieve adequate performance on PEM fuel cell. The SEM scans showed the quality and reproducibility of the spraying technique.

The PBI membrane-electrode assemblies were tested in the fuel cell test station without the need for humidification of reactant gases. During the study, it was achieved to operate the single cell up to 160°C. The observed maximum power output was increased considerably from 0.015 to 0.072 W/cm^2 at 150°C when the binder of the catalyst was changed from PBI to PBI and PVDF mixture (PVDF : PBI = 3 : 1). The maximum power output reached for the cell increased two times when the fuel cell operating temperature was increased from 125°C to 160°C. The OCV values were quite satisfactory which were around 1 V.

References

1. Barbir, F. PEM Fuel Cells: Theory and Practice; Elsevier Academic Press: Burlington, 2005.
2. Li, Q.; He, R.; Jensen, J. O.; Bjerrum, N. J. Fuel Cells 2004, 4, 147.
3. Li, Q.; He, R.; Jensen, J. O.; Bjerrum, N. J. Chem Mater 2003, 15, 4896.
4. Ma, Y. PhD Thesis; Case Western Reserve University: Ohio, 2004.
5. Xiao, L.; Zhang, H.; Scanlon, E.; Ramanathan, L. S.; Choe, E.; Rogers, D.; Apple, T.; Benicewicz, B. C. Chem Mater 2005, 17, 5328.
6. Schönberger, F.; He, M.; Kerres, J. Solid State Ionics 2007, 178, 547.
7. Vogel, H.; Marvel, C. S. J Polym Sci 1961, 50, 511.
8. Iwakura, Y.; Uno, K.; Imal, Y. J Polym Sci Part A: Polym Chem 1964, 2, 2605.
9. Schuster, M. F. H.; Meyer, W. H.; Schuster, M.; Kreuer, K. D. Chem Mater 2004, 16, 329.
10. Xing, B. Z.; Savadogo, O. J New Mater Electrochem Syst 1999, 2, 95.
11. Kongstein, O. E.; Berning, T.; Borresen, B.; Seland, F.; Tunold, R. Energy 2007, 32, 418.

12. Wainright, J. S.; Wang, J. T.; Weng, D.; Savinell, R. F.; Litt, M. J Electrochem Soc 1995, 142, L121.
13. Kim, J. H.; Kim, H. J.; Lim, T. H.; Ho, I. L. J Power Sources 2007, 170, 275.
14. Lobato, J., Rodrigo, M. A.; Linares, J. J.; Scott, K. J Power Sources 2006, 157, 284.
15. Ergun, D.; Erkan, S.; Devrim, Y.; Bac, N.; Eroglu, I. Proceedings of HYPOTHESIS VIII; Lisbon, 2009.
16. Shogbon, C. B.; Brousseau, J.; Zhang, H.; Benicewicz, B. C.; Akpalu, Y. A. Macromolecules 2006, 36, 9409.
17. Buckley, A.; Stuetz, D.; Serad, G. A. Encyclopedia of Polymer Science and Engineering; Wiley: New York, 1987.
18. Buckley, A.; Stuetz, D. E.; Serad, G. A. In Encyclopedia of Polymer Science and Engineering, Mark, H. F.; Bikales, N.; Overberger, C. G.; Menges, C.; Kroschwitz, J. I., Eds.; Wiley: New York, 1988; Vol. 11, p 572.
19. Mark, J. E., Eds. Polymer Data Handbook; Oxford University Press: New York, 1999.
20. Asensio, J. A.; Borro's, S.; Romero, P. G. J Electrochem Soc 2004, 151, A304.
21. He, R.; Li, Q.; Bach, A.; Jensen, J. O. J Membr Sci 2006, 277, 38.
22. Wereta, A.; Gehatia, M. T. Polym Eng Sci 1978, 18, 204.
23. Elashmawi, I. S. Mater Chem Phys 2008, 107, 96.
24. Carollo, A.; Quartarone, E.; Tomasi, C. J Power Sources 2006, 160, 175.
25. Lobato, J.; Canizares, P.; Rodrigo, M. A.; Linares, J. J.; Manjavacas G. J Membr Sci 2006, 280, 351.
26. Stevens, M. P. Polymer Chemistry: An Introduction; Oxford University Press: New York, 1999.
27. Wainright, J. S.; Litt, M. H.; Savinell, R. F. Handbook of Fuel Cells, Fundamentals, Technology and Applications; Wiley: New York, 2003.
28. Li, Q.; Hjuler, H. A.; Bjerrum, N. J. J Appl Electrochem 2001, 31, 773.
29. Hasiotis, C.; Qingfeng, L.; Deimede, V.; Kallitsis, J. K.; Kontoyannis, C. G.; Bjerrum, N. J. J Electrochem Soc. 2001, 148, A513.
30. Bjerrum, N. J.; Li, Q.; Hjuler, H. A. World Pat. WO 0,118,894A2 (2001).
31. Seland, F.; Berning, T.; Borresen, B.; Tunold, R. J Power Sources 2006, 160, 27.
32. Kundu, S.; Fowler, M. W.; Simona, L. C.; Grot, S. J Power Sources 2006, 157, 650.
33. Park, S. B.; Kim, S., Park, Y.; Oh, M. J Phys Conf Ser 2009, 165, 012046.
34. Rangel, C. M.; Silva, R. A.; Paiva, T. I. J New Mater Electrochem Syst 2009, 12, 119.
35. Liu, G.; Zhang, H.; Hua, J.; Zhai, Y.; Xua, D., Shao, Z. J Power Sources 2006, 162, 547.
36. Barbir, F. In Handbook of Fuel Cell Technology—Fundamentals, Technology and Applications; Vielstich, W.; Lamm, A.; Gasteiger, H., Eds.; Wiley: New York, 2003; Vol.4, Part 3, p 683.
37. Lobato, J.; Canizares, P.; Rodrigo, M. A., Linares, J. J.; Pinar, F. J. Int J Hydrogen Energy 2010, 35, 1347.
38. Zhang, J.; Tang, Y.; Song, C. J Power Sources 2007, 172, 163.
39. Wang, J. T.; Savinell, R. F.; Wainright, J.; Litt, M., Yu, H. Electrochim Acta 1996, 41, 193.
40. Savadogo, O.; Xing, B. J New Mater Electrochem Syst 2000, 3, 343.
41. Li, Q.; Hjuler, H. A.; Hasiotis, C.; Kallitsis, J. K.; Kontoyannis, C. G.; Bjerrum, N. J. Electrochem Solid State Lett 2002, 5, A125.